



Metal–organic frameworks HKUST-1 for liquid-phase adsorption of uranium



Yafei Feng^a, Heng Jiang^b, Songnan Li^a, Jun Wang^a, Xiaoyan Jing^a, Yuren Wang^{b,*}, Meng Chen^b

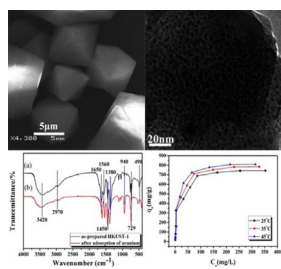
^a Key Laboratory of Super-light Materials & Surface Technology, Ministry of Education, Harbin Engineering University, Harbin 150001, People's Republic of China

^b Key Laboratory of Microgravity Science, Institute of Mechanics, Chinese Academy of Sciences, Beijing 100190, People's Republic of China

HIGHLIGHTS

- Synthesis of the HKUST-1 with mesoporous structure.
- Exploration of the new application of MOFs materials in uranium removal.
- Development of a high-efficiency adsorbent for uranium.

GRAPHICAL ABSTRACT



ARTICLE INFO

Article history:

Received 4 December 2012

Received in revised form 21 March 2013

Accepted 12 April 2013

Available online 25 April 2013

Keywords:

Metal–organic frameworks
HKUST-1
Liquid-phase adsorption
Uranium

ABSTRACT

This paper reports on the efficient adsorption for uranium by metal–organic frameworks (MOFs) HKUST-1 from aqueous solution. The structure of the prepared HKUST-1 was characterized by X-ray diffraction (XRD), Scanning electron microscope (SEM), Transmission electron microscope (TEM), Fourier transform infrared spectroscopy (FTIR) and nitrogen adsorption/desorption analysis. The influences of different experimental parameters were studied, such as initial solution pH, adsorbent dosage, adsorption time, temperature and various concentrations of uranium uptake. The thermodynamic parameters including Gibbs free energy (ΔG°), standard enthalpy change (ΔH°) and standard entropy change (ΔS°) for the process were calculated using the Langmuir constants. The results showed that the equilibrium data fitted well to Langmuir model in the studied range of uranium concentration (10 mg/L–800 mg/L) and temperature (298 K–318 K), and the HKUST-1 exhibited the highest uptake for uranium at 318 K, at the initial solution pH value of 6 and at the initial uranium concentration of 800 mg/L. The thermodynamics of uranium/HKUST-1 system indicated the spontaneous and endothermic nature of the process. And the kinetics of the adsorption process followed the pseudo-second-order kinetics model.

© 2013 Elsevier B.V. All rights reserved.

1. Introduction

Uranium is a naturally radioactive element and harmful to health. Its existence in water is often the most significant way of exposure to humans [1]. Thus, it is very important to realize efficient removal of uranium from water. The methods of

recovering uranium from water commonly include chemical precipitation, electrochemical treatments, membrane separation, ion exchange, intracellular sequestration and adsorption [2]. Among these methods, adsorption is the most attractive and effective way to remove uranium from aqueous solution, owing to its low cost, flexible design and insensitivity to toxic pollutants. Hence, various materials have been developed for uranium adsorption, such as metal oxides, carbon, zeolite, and biomaterials [3].

As promising adsorption materials, metal–organic frameworks (MOFs) consisting of clusters or chains of metal ions connected by

* Corresponding author. Tel.: +86 010 82544091; fax: +86 010 82544096.

E-mail address: yurenwang@imech.ac.cn (Y. Wang).

organic ligands have attracted enormous research interest in recent decade. Many reports on gas adsorption properties of MOFs have been given to date, such as H₂, N₂, O₂, CO, CO₂, N₂O, CH₄, ethylene, ethane, n-dodecane and n-butane [4,5]. More recently, studies on liquid phase adsorption of highly water-stable MOFs have been paid more attention [6–8]. For example, Alaerts et al. have studied a batch of liquid phase adsorption experiments on MOFs and pointed out that MOFs can be served as high-efficiency adsorbents for some aromatic compounds and organic contaminants [9]. Moreover, the adsorption and removal of pharmaceuticals, dyes and sulfur compounds from liquid phase by MOFs have also been reported [10–12]. All the studies have strongly proved that MOFs can be as superior candidate materials either in gas adsorption or in liquid phase adsorption. Compared to conventional adsorbent, MOFs have possessed several advantages, such as rich topological structure, mild synthetical conditions and avoidable post-synthetic calcinations steps [13]. However, to the best of our knowledge, rarely studies on the adsorption of uranium on MOFs have been done so far. The purpose of this paper is two-fold. The first purpose aims to explore the application of MOFs materials in liquid-phase adsorption. The second purpose is to develop an efficient adsorbent of uranium.

In this paper, HKUST-1 (Cu₃(BTC)₂) with mesoporous structure was prepared by solvothermal technique. In the framework of this material, two octahedrally coordinated Cu atoms are connected to eight oxygen atoms of tetra-carboxylate units to form a dimeric Cu paddle wheel. Each BTC ligand holds three dimeric Cu paddle wheels to form an open framework with face-centered cubic symmetry [14]. We investigated the influence of various experimental parameters on uranyl adsorption and to determine the optimum procedure for the separation of uranyl from solution by adsorption on HKUST-1 with mesoporous structure. Adsorption isotherms were analyzed by Langmuir and Freundlich. The thermodynamic parameters, such as ΔG⁰, ΔH⁰ and ΔS⁰, were calculated and interpreted. The kinetics was studied by the pseudo-first-order and the pseudo-second-order models. And the adsorption mechanisms were attempted to explain.

2. Materials and methods

2.1. Preparation

The as-prepared HKUST-1 was synthesized by taking the method reported by Cao as a reference [15]. Details of the preparation procedure are: Cu(NO₃)₂·3H₂O (5 g, 0.021 mol) and H₃BTC (2.5 g, 0.012 mol) were dissolved in 300 ml of solvent consisting of equal amounts of DMF, ethanol and deionized water by ultraso- nication. The solution was placed in an oven and heated to 358 K for 20 h. The blue product was isolated, rinsed with 50 ml DMF for three times and immersed in absolute ethanol every 24 h for 72 h. Finally, the blue product was heated to 393 K for 24 h in vacuum.

2.2. Characterization

The HKUST-1 powders were analyzed by using a Rigaku Ultima IV X-ray powder diffractometer with a Cu Kα1 radiation source ($k = 1.54056 \text{ \AA}$) operated at 40 kV and 40 mA at a scanning step of 0.01° in the 2θ range 5°–50°. Fourier-transform infrared (FT-IR) spectra were recorded with an AVATAR 360 FT-IR spectrophotometer using a standard KBr pellet technique and morphologies were characterized using a JEOL JSM-6480A Scanning electron microscope and a PHILIPS CM 200 FEG Transmission electron microscope. Thermogravimetric analysis (TGA) data were obtained on a TA TGA Q5000IR under N₂ stream with a heating rate of 5 °C min⁻¹ from room temperature to 400 °C. The porosity was measured with a Micromeritics ASAP 2020 gas sorption and porosimetry apparatus

using nitrogen gas at 77 K. Before the measurements, the sample (0.1 g) was heated at 110 °C under vacuum for 10 h.

2.3. Adsorption experiments

All adsorption studies were carried out in a series of 100 ml conical flasks containing a given dose of adsorbents together with 50 ml water solution of uranium in a thermostatic water shaker. Batch equilibrium isotherms experiments on HKUST-1 were conducted with a range (10–800 mg/L, details were shown in related captions) of different concentrations of uranium solutions by contacting a constant mass (0.03 g) of HKUST-1 for a period of 2 h at 25, 35, 45 ± 1 °C, using the maximum shaking rate of 200 rpm. After equilibration, HKUST-1 was separated from the solution by filtration and the effluent was analyzed using a Trace Uranium Analyzer.

The amount of the uranium loading (mg) per unit mass of HKUST-1, q_e , and the % removal of uranium were obtained by Eqs. (1) and (2), respectively:

$$q_e = (C_0 - C_e) \frac{V}{m} \quad (1)$$

$$\text{Removal(\%)} = 100 \times \frac{C_0 - C_e}{C_0} \quad (2)$$

where C_0 and C_e are initial and equilibrium concentrations in mg/L, m is the mass of adsorbent in grams, and V is the volume of solution in liters.

2.4. Desorption experiments

Desorption studies were carried out by using different eluants, such as NaHCO₃, NH₄HCO₃, Na₂CO₃, NaOH, NaCl, NaNO₃, HNO₃, H₂SO₄, HCl and distilled water. Desorption process was divided into two parts. Firstly, the adsorption of uranium on HKUST-1 was carried out with the adsorbent dosage of 0.03 g in a 50 ml uranium solution of 500 mg/L for 2 h of contact at 25 °C. When the adsorption equilibrium was reached, the supernatants were separated for analyzing the residual uranium. Secondly, the filtered solid residue was dried at 80 °C. And then 10 ml of the selected eluant was used for desorption of uranium from the uranium-loaded HKUST-1(0.035 g). The mixture was stirred for 2 h before subsequent analyses were performed.

3. Results and discussion

3.1. Characterization of the prepared HKUST-1

Fig. 1(a) shows the XRD patterns of the resulting products. All of the diffraction peaks can be indexed to crystalline HKUST-1 [16], and no obvious peaks of impurities can be detected in the XRD patterns. Small variations in intensity can be ascribed to a different degree of hydration [14]. Moreover, sharpness and high intensity of peaks indicate high crystallinity of the prepared bulk materials, which is in accordance with the SEM image of the prepared HKUST-1. The typical morphology of HKUST-1 can be seen in **Fig. 1(c)**, these crystals have well-shaped octahedra. The TEM image of the prepared HKUST-1 reveals the porous structure (**Fig. 1(d)**). The existence of mesoporous can be further demonstrated by the presence of a hysteresis loop at relative high pressure in the nitrogen adsorption/desorption analysis. The calculated average mesopore diameter by BJH method is about 13.5 nm and mesopore distribution is in a wide range (**Fig. 1(b)** and its inset). The TGA curve is reported in **Fig. S1**. This first weight loss is due to the loss of ethanol and water. After a plateau, a second step of weight loss takes place after 298 °C and corresponds to the structural decomposition [14,17]. The TGA data reveal that the HKUST-1 is stable

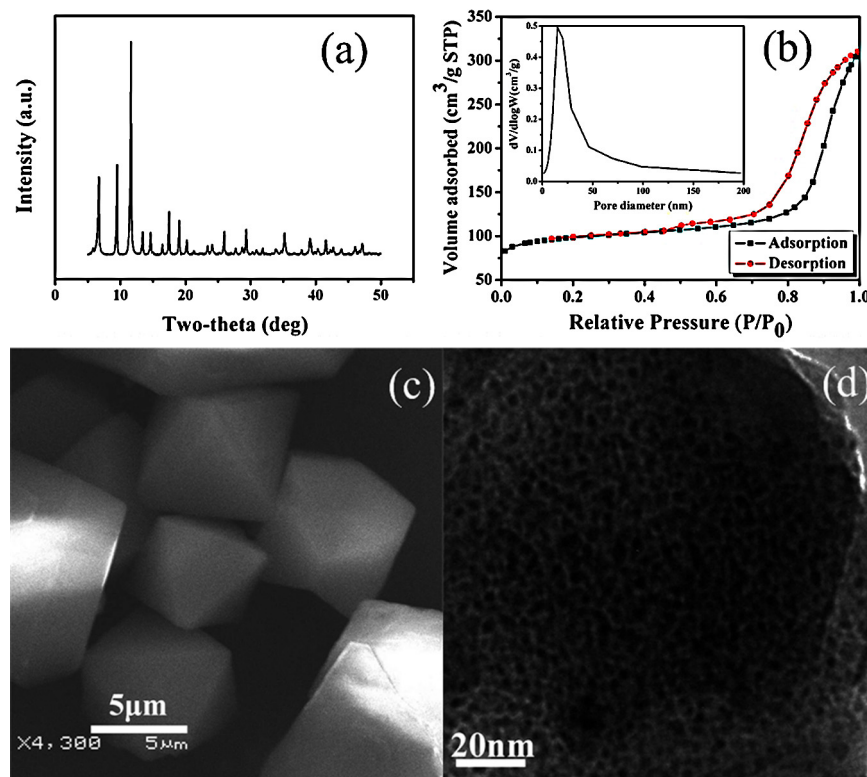


Fig. 1. Characterization of as-prepared HKUST-1 (a) XRD patterns of as-prepared HKUST-1, (b) N_2 adsorption/desorption isotherms of as-prepared HKUST-1. Inset shows pore size distribution of the as-prepared HKUST-1 calculated by BJH method, (c) SEM image of as-prepared HKUST-1, (d) TEM image of as-prepared HKUST-1.

up to 298 °C. The FT-IR patterns of as-prepared HKUST-1 before and after adsorption are shown in Fig. S2. And the presence of a broad and strong peak at 3210–3630 cm^{-1} is assigned to $\nu(\text{H}_2\text{O})$. The peak of 2970 cm^{-1} is associated with $\nu(\text{C}-\text{H})$ of the DMF molecules [18]. The peak of 1650 cm^{-1} is assigned to $\nu(\text{C}=\text{O})$ of the deprotonated benzene tricarboxylic acid [19]. And the IR absorption bands in the 1300–1500 and 1500–1700 cm^{-1} ranges are due to $\nu_{\text{sym}}(\text{C}-\text{O}_2)$ and $\nu_{\text{asym}}(\text{C}-\text{O}_2)$ stretching modes, respectively. IR bands around 700 cm^{-1} and 1450 cm^{-1} are due to $\nu(\text{C}-\text{H})$ bending mode and a combination of benzene ring stretching and deformation modes. The absorption bands around 500 cm^{-1} are assigned to Cu-O stretching modes [20].

3.2. Influence of initial pH values

The effect of initial pH values on the adsorption of uranium on HKUST-1 was studied by using 50 ml of uranium solutions 200 mg/L and 0.05 g HKUST-1 at pH 2.0–10.0 at 25 °C for 120 min (Fig. 2) and the influence of the initial pH on the adsorption of uranium from water was shown in Table 1. As shown in Fig. 2, with the increase of pH value, the removal rate of uranium gradually reached the maximum (99.6%, pH = 6) and decreased to 99.1% at pH 8, and then steeply decreased to 68.9% at pH 10. On the basis of an electrostatic interaction model [21] and uranium species in uranium

solutions with different pH values [22], the influence of pH on uranium removal was attempted to explain. At low pH values, the predominant species was uranyl (UO_2^{2+}). Under near-neutral condition, UO_2^{2+} , $\text{UO}_2(\text{OH})^+$ and $\text{UO}_2(\text{OH})_2^{2+}$ dominated. As the pH increased, the adsorbent surface became more negatively charged and therefore the adsorption of positively charged uranium species was more favorable. In addition, the reduction of H^+ ions also facilitated preferential adsorption of uranium species. At alkaline pH values, the removal rate decreased probably due to the presence of $[\text{UO}_2(\text{CO}_3)_2]^{2-}$ and $[\text{UO}_2(\text{CO}_3)_3]^{4-}$. Hence, the optimum pH 6 was used for further experiments.

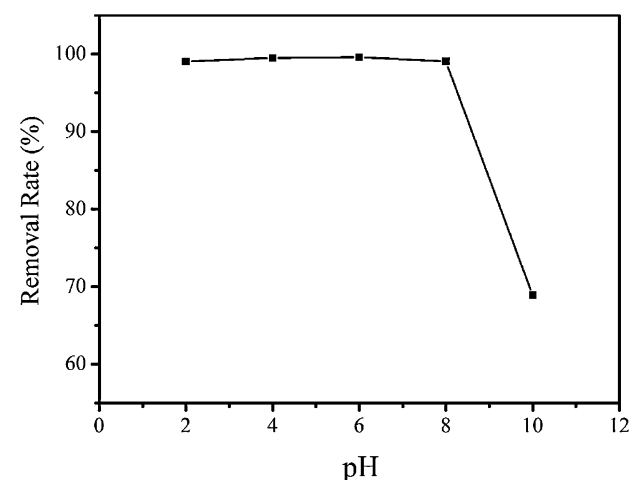


Fig. 2. Effect of initial pH on adsorption of uranium by HKUST-1 (Adsorption dosage 0.05 g, $C_0 = 200 \text{ mg/L}$, agitation time 2 h, $T = 25^\circ\text{C}$ and pH = 2–10).

Table 1

Effect of initial pH on the adsorption of uranium by HKUST-1.

| pH initial | % Adsorbed |
|------------|------------|
| 2 | 99.05 |
| 4 | 99.53 |
| 6 | 99.62 |
| 8 | 99.07 |
| 10 | 68.88 |

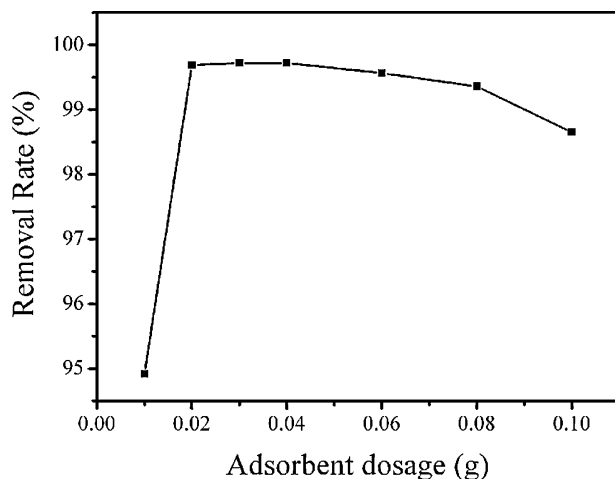


Fig. 3. Effect of solid/liquid ratio on adsorption of uranium by HKUST-1 (Adsorption dosage 0.01–0.1 g, $C_0 = 200 \text{ mg/L}$, agitation time 2 h, $T = 25^\circ\text{C}$ and pH = 6).

3.3. Influence of dosage of HKUST-1

The effect of different dosage of HKUST-1 on the uranium removal was studied by using 50 ml solution (pH = 6) with initial uranium concentration of 200 mg/L. As shown in Fig. 3, the removal rate of uranium steeply increased with the increasing dosage of HKUST-1 and reached the maximum (99.7%) at the dosage of HKUST-1 0.03 g. It was due to enhanced active sites with the increasing amount of HKUST-1. When the dosage of HKUST-1 exceeded 0.04 g, the removal rate of uranium gradually decreased to 98.7%. And the decrease was likely due to the agglomeration of the HKUST-1 particles, resulting in hindering the adsorption of ions in solution on the surface of adsorbents. Hence, an adsorption dosage of 0.03 g was selected for the following studies.

3.4. Adsorption isotherms

Adsorption isotherms were used to describe adsorption mechanism of adsorbent for adsorbate [23,24]. The adsorption isotherms of uranium on HKUST-1 at the temperature of 25 °C, 35 °C, 45 °C were shown in Fig. 4. The equilibrium adsorption of uranium on HKUST-1 increased from 744 mg/g to 810 mg/g when temperature increased from 298 to 318 K. The result suggested that uranium removal by adsorption on HKUST-1 obviously favored a higher temperature when the initial uranium concentration exceeded 200 mg/g. Freundlich and Langmuir isotherm equations were commonly adopted to fit the isothermal adsorption processes of adsorbent for adsorbate. Freundlich and Langmuir equations and isotherm parameters displayed in Table 2. The fitting curves of all the adsorption data to both isotherm models were depicted in Figs. S3 and S4. And the constants of isotherms and correlation coefficient values of Freundlich and Langmuir were given in Table 3. It was clearly shown that the correlation coefficients of Langmuir isotherm model ($R^2 = 0.998, 0.998, 0.999$) were higher than those of Freundlich ($R^2 = 0.884, 0.837, 0.855$). Hence, Langmuir isotherm yielded better fit to the experimental data within the studied

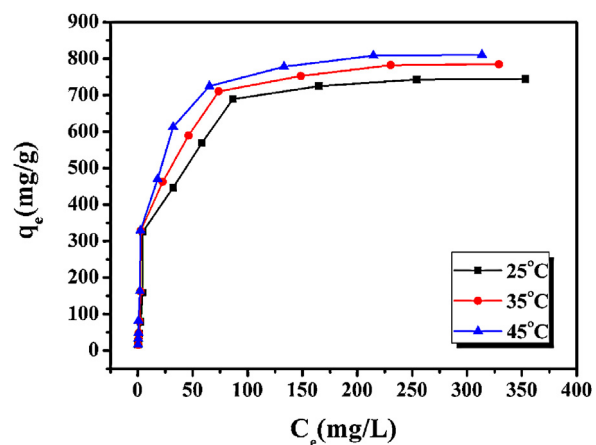


Fig. 4. Effect of uranium concentration on the adsorption of uranium by HKUST-1 (Adsorption dosage 0.03 g, $C_0 = 10, 20, 30, 50, 100, 200, 300, 400, 500, 600, 700, 800 \text{ mg/L}$, agitation time 2 h, $T = 25\text{--}45^\circ\text{C}$ and pH = 6).

Table 2
Isotherm models, equations and parameters of adsorption.

| Isotherm model | Isotherm equation | Isotherm parameter |
|----------------|------------------------------------|--|
| Freundlich | $\lg q_e = \lg K_f + 1/n \lg C_e$ | C_e (mg/L): the equilibrium concentration in the solution q_e (mg/g): the amount adsorbed on the adsorbent at equilibrium K_f [(mg/g)(L/mg) n]: the Freundlich constant denoting as the adsorption capacity of the adsorbent |
| Langmuir | $1/q_e = (q_0 b C_e)^{-1} + 1/q_0$ | n : the adsorption intensity parameter q_0 (mg/g): the maximum adsorption capacity b (L/mg): a constant related to the adsorption energy |

temperature range (25–45 °C). The result suggested that adsorption mechanism was monolayer coverage on the surface of the adsorbent [24]. In addition, the values of q_0 evaluated from Langmuir model were close to the experimental values of q_e at the initial uranium concentration of 800 mg/g. The K_f indicating the adsorption capacity of the adsorbent increased with an increase temperature, which was consistent with the results of Langmuir model. And the values of $1 < n < 10$ showed favorable adsorption of uranium onto adsorbents.

3.5. Adsorption thermodynamics

In environmental engineering practice, both the energy and entropy factors must be considered in order to determine which process will occur spontaneously. Variety of the Gibbs free energy (ΔG^0) is the fundamental criterion of spontaneity. The equations used to calculate ΔG^0 , ΔS^0 , ΔH^0 and the parameters of adsorption thermodynamics displayed in Table 4. ΔS^0 and ΔH^0 were calculated from Van't Hoff's plot (Fig. 5) and the calculated ther-

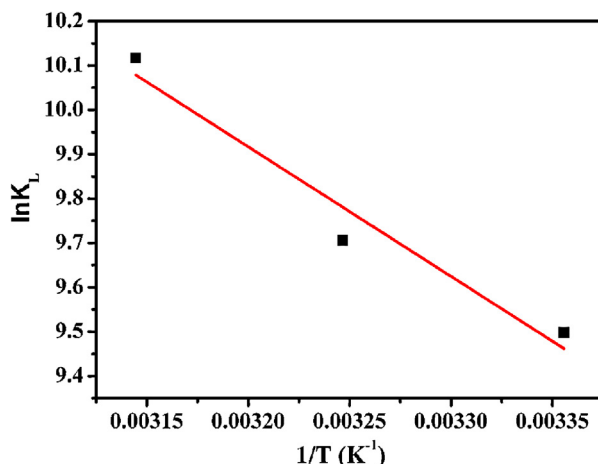
Table 3
Isotherm parameters for adsorption of uranium on HKUST-1.

| Temp(°C) | Langmuir | | | | | Freundlich | | | | |
|----------|--------------|------------|-------|---------------|------------|------------|-------|-------|-------|-------|
| | q_0 (mg/g) | b (L/mg) | R^2 | K_L (L/mol) | $\ln(K_f)$ | SD | K_f | n | R^2 | SD |
| 25 | 787.4 | 0.056 | 0.998 | 13,328 | 9.498 | 0.007 | 50.22 | 1.834 | 0.884 | 0.206 |
| 35 | 826.4 | 0.069 | 0.998 | 16422 | 9.706 | 0.006 | 60.54 | 1.884 | 0.837 | 0.246 |
| 45 | 840.3 | 0.104 | 0.999 | 24752 | 10.117 | 0.004 | 77.21 | 1.996 | 0.855 | 0.234 |

Table 4

Equations and parameters of adsorption thermodynamics.

| Equation | Thermodynamics parameter |
|--|---|
| $\Delta G^0 = -RT \ln K_L$ | R : the gas constant (8.314 J/mol K) T : the temperature in K K_L : the Langmuir equilibrium constant |
| $\ln K_L = \Delta S^0/R - \Delta H^0/RT$ | ΔG^0 : Gibbs free energy (kJ/mol) ΔH^0 : standard enthalpy change (kJ/mol) ΔS^0 : standard entropy change (J/mol/K) |

**Fig. 5.** Van't Hoff plot for removal of uranium by HKUST-1.

modynamics parameters were represented in Table 5. The positive value of standard enthalpy (ΔH^0) of adsorption suggested the endothermic nature of the adsorption of uranium on HKUST-1. The negative standard free energy (ΔG^0) indicated that the adsorption reaction was a spontaneous process. And the positive standard entropy (ΔS^0) implied that the driving force for the adsorption of uranium on HKUST-1 was controlled by an entropy effect rather than an enthalpy change.

3.6. Effect of reaction time

The effect of agitation time on uranium adsorption experiments was shown in Fig. S5. The amount of adsorbed uranium increased with an increase of agitation time and reached equilibrium after 60 min. The kinetic process of uranium adsorption consisted of an initial rapid phase and a plateau region. Initial rapid phase was interpreted to be the instantaneous adsorption stage or external surface adsorption. The plateau region was the gradual adsorption stage where intraparticle diffusion controlled the adsorption rate until finally the uptake reached equilibrium [1].

3.7. Adsorption kinetics

Adsorption kinetics was mainly used to investigate diffusion mechanism, adsorbed control step and influencing factors of adsorbed velocity [25,26]. The adsorption data were fitted to the pseudo-first-order kinetic model and the pseudo-second-order

Table 5

Calculated thermodynamics parameters for adsorption of uranium on HKUST-1.

| Temp (°C) | ΔG^0 (kJ/mol) | ΔH^0 (kJ/mol) | ΔS^0 (J/mol/K) |
|-----------|-----------------------|-----------------------|------------------------|
| 25 | -23.5 | 24.3 | 160.3 |
| 35 | -24.9 | | |
| 45 | -26.7 | | |

Table 6

Kinetic models, equations and parameters of adsorption.

| Kinetic model | Kinetic equation | Kinetic parameter |
|---------------------|------------------------------------|--|
| pseudo-first-order | $\ln(q_e - q_t) = \ln q_e - k_1 t$ | q_e (mg/g): the amount of uranium adsorbed at equilibrium q_t (mg/g): the amount of uranium adsorbed at time t |
| pseudo-second-order | $t/q_t = (k_2 q_e^2)^{-1} + t/q_e$ | k_1 (min ⁻¹): the pseudo-first-order rate constant k_2 (g mg ⁻¹ min ⁻¹): the pseudo-second-order rate constant t (min): reaction time |

kinetic model, respectively. And the kinetic equations of the two models were listed in Table 6. The kinetic parameters of uranium adsorption by HKUST-1 were calculated from Figs. S6 and S7, and were shown in Table 7. The results showed that the correlation coefficients for the pseudo-second-order kinetic model were equal to 1 for all the temperatures and the theoretical values of q_e also agreed very well with the experimental ones. This suggested that the pseudo-second-order gave a satisfactory fit to all of the experimental data. And the results indicated that the rate-controlling step might be chemical sorption or chemisorption involving valency forces through sharing or exchange of electrons between adsorbent and adsorbate [27]. Moreover, the fitting curves of the pseudo-second-order model had the same slope under the studied temperatures, which indicated temperature within the studied range had no obvious influence on the equilibrium adsorption capacity of the HKUST-1 when the initial uranium concentration was low.

3.8. Mechanism

As stated above, HKUST-1 consisted of Cu²⁺ ions connected by BTC ligand. And each BTC ligand contained three carboxyl groups. Hence, a great number of oxygen atoms in these carboxyl groups provided coordination sites for uranium species [28]. As shown in Fig. S2, the presence of a strong band at 940 cm⁻¹ displayed $\nu(U=O)$ stretch and the IR bands of functional groups containing oxygen shifted [29]. In addition, although the framework was electrical neutral, partial negative charges localized on the carboxylate units [30]. And uranium was always present in the form of positive ions under near-neutral condition, such as UO₂(OH)⁺ and UO₂²⁺. All these suggested that the adsorption properties of HKUST-1 were supposed to be determined not only by coordination, but also by Coulomb electrostatic interactions. Meanwhile, the Cu²⁺ sites had high affinity for water [31], resulting in high dispersity of HKUST-1 in water, which was beneficial to uranium adsorption. Moreover, owing to efficient mass transport, the mesoporous

Table 7

Kinetic parameters of uranium adsorption by HKUST-1.

| Parameters | 25 | 35 | 45 |
|---|----------|----------|----------|
| Temperature (°C) | 25 | 35 | 45 |
| q_e (mg/g) ($C_e = 200$ mg/L) | 332.0 | 332.2 | 332.5 |
| pseudo-first-order | | | |
| k_1 (min ⁻¹) | 0.07315 | 0.06014 | 0.15404 |
| R^2 | 0.83 | 0.57 | 0.94 |
| SD | 1.012 | 1.312 | 0.531 |
| q_e (cal) (mg/g) | 1.97 | 1.32 | 4.67 |
| pseudo-second-order | | | |
| k_2 (g mg ⁻¹ min ⁻¹) | 0.17462 | 0.15245 | 0.19679 |
| R^2 | 1 | 1 | 1 |
| SD | 0.000059 | 0.000036 | 0.000043 |
| q_e (cal) (mg/g) | 332.2 | 332.2 | 332.2 |

structure in HKUST-1 played a significant role in enhancing the adsorption capacity of HKUST-1 [32–35].

3.9. Desorption

In order to estimate the reversibility, desorption of uranium from HKUST-1 using different eluants was investigated. After adsorption of uranium onto HKUST-1, HKUST-1 was treated with different desorptive solutions to recover the adsorbed uranium from HKUST-1 (Table S1). But HKUST-1 showed the lower desorption yield, owing to chemical adsorption.

4. Conclusions

In summary, HKUST-1 with mesoporous exhibited high adsorption capacity for uranium from aqueous solution. The optimal adsorption conditions were confirmed, including the solution pH (at 6), dosage (0.03 g) of adsorbents and the agitation time (2 h). And temperature had no obvious effect on the adsorption process when the initial uranium concentration was below 200 mg/g, but the adsorption obviously favored a higher temperature when the initial uranium concentration exceeded 200 mg/g. The HKUST-1 exhibited the highest uptake capacity for uranium at 318 K, at the initial solution pH value of 6 and at the initial uranium concentration of 800 mg/L. Langmuir adsorption isotherm was found to be more suitable to explain the adsorption of uranium onto HKUST-1 and the adsorption kinetics data matched with the pseudo-second-order model. The thermodynamics of uranium/HKUST-1 system indicated the spontaneous and endothermic nature of the process.

Acknowledgments

The work wishes to acknowledge the support from the National Basic Research Program of China (973 Program, No. 2011CB710901) and the Fundamental Research Funds of the Central University (HEUCFZ).

Appendix A. Supplementary data

Supplementary data associated with this article can be found, in the online version, at <http://dx.doi.org/10.1016/j.colsurfa.2013.04.032>.

References

- [1] R. Han, W. Zou, Y. Wang, L. Zhu, Removal of uranium (VI) from aqueous solutions by manganese oxide coated zeolite: discussion of adsorption isotherms and pH effect, *J. Environ. Radioact.* 93 (2007) 127–143.
- [2] M. Kalin, W.N. Wheeler, G. Meinrath, The removal of uranium from mining waste water using algal/microbial biomass, *J. Environ. Radioact.* 78 (2004) 151–177.
- [3] M. Rafatullah, O. Sulaiman, R. Hashim, A. Ahmad, Adsorption of methylene blue on low-cost adsorbents: a review, *J. Hazard. Mater.* 177 (2010) 70–80.
- [4] J. Liu, J.T. Culp, S. Natesakhawat, B.C. Bockrath, B. Zandie, S.G. Sankar, G. Garberoglio, J.K. Johnson, Experimental and theoretical studies of gas adsorption in Cu₃(BTC)₂: an effective activation procedure, *J. Phys. Chem. C* 111 (2007) 9305–9313.
- [5] N. Klein, A. Henschel, S. Kaskel, n-Butane adsorption on Cu₃(btc)₂ and MIL-101, *Microporous Mesoporous Mater.* 129 (2010) 238–242.
- [6] A. Henschel, I. Senkovska, S. Kaskel, Liquid-phase adsorption on metal-organic frameworks, *Adsorption* 17 (2011) 219–226.
- [7] W. Xuan, C. Zhu, Y. Liu, Y. Cui, Mesoporous metal-organic framework materials, *Chem. Soc. Rev.* 41 (2012) 1677–1695.
- [8] X.X. Huang, L.G. Qiu, W. Zhang, Y.P. Yuan, X. Jiang, A.J. Xie, Y.H. Shen, J.F. Zhu, Hierarchically mesostructured MIL-101 metal-organic frameworks: supramolecular template-directed synthesis and accelerated adsorption kinetics for dye removal, *CrystEngComm* 14 (2012) 1613–1617.
- [9] L. Alaerts, M. Maes, M.A. van der Veen, P.A. Jacobs, D.E. De Vos, Metal-organic frameworks as high-potential adsorbents for liquid-phase separations of olefins, alkylnaphthalenes and dichlorobenzenes, *Phys. Chem. Chem. Phys.* 11 (2009) 2903–2911.
- [10] K.A. Cychosz, A.J. Matzger, Water stability of microporous coordination polymers and the adsorption of pharmaceuticals from water, *Langmuir* 26 (2010) 17198–17202.
- [11] E. Haque, J.W. Jun, S.H. Jhung, Adsorptive removal of methyl orange and methylene blue from aqueous solution with a metal-organic framework material, iron terephthalate (MOF-235), *J. Hazard. Mater.* 185 (2011) 507–511.
- [12] K.A. Cychosz, A.G. Wong-Foy, A.J. Matzger, Liquid phase adsorption by microporous coordination polymers: removal of organosulfur compounds, *J. Am. Chem. Soc.* 130 (2008) 6938–6939.
- [13] J. Juan-Alcañiz, J. Gascon, F. Kapteijn, Metal-organic frameworks as scaffolds for the encapsulation of active species: state of the art and future perspectives, *J. Mater. Chem.* 22 (2012) 10102–10118.
- [14] K. Schlichte, T. Kratzke, S. Kaskel, Improved synthesis, thermal stability and catalytic properties of the metal-organic framework compound Cu₃(BTC)₂, *Microporous Mesoporous Mater.* 73 (2004) 81–88.
- [15] Z. Xiang, X. Peng, X. Cheng, X. Li, D. Cao, CNT@Cu₃(BTC)₂ and metal-organic frameworks for separation of CO₂/CH₄ mixture, *J. Phys. Chem. C* 115 (2011) 19864–19871.
- [16] Z.Q. Li, L.G. Qiu, T. Xu, Y. Wu, W. Wang, Z.Y. Wu, X. Jiang, Ultrasonic synthesis of the microporous metal-organic framework Cu₃(BTC)₂ at ambient temperature and pressure: an efficient and environmentally friendly method, *Mater. Lett.* 63 (2009) 78–80.
- [17] Y.K. Seo, G. Hundal, I.T. Jang, Y.K. Hwang, C.H. Jun, J.S. Chang, Microwave synthesis of hybrid inorganic–organic materials including porous Cu₃(BTC)₂ from Cu(II)-trimesate mixture, *Microporous Mesoporous Mater.* 119 (2009) 331–337.
- [18] Z. Xiang, D. Cao, X. Shao, W. Wang, J. Zhang, W. Wu, Facile preparation of high-capacity hydrogen storage metal-organic frameworks: a combination of microwave-assisted solvothermal synthesis and supercritical activation, *Chem. Eng. Sci.* 65 (2010) 3140–3146.
- [19] R. Senthil Kumar, S. Senthil Kumar, M. Anbu kulandainathan, Efficient electroynthesis of highly active Cu₃(BTC)₂-MOF and its catalytic application to chemical reduction, *Microporous Mesoporous Mater.* 168 (2013) 57–64.
- [20] E. Borfecchia, S. Maurelli, D. Gianolio, E. Groppo, M. Chiesa, F. Bonino, C. Lamberti, Insights into adsorption of NH₃ on HKUST-1 metal-organic framework: a multitechnique approach, *J. Phys. Chem. C* 116 (2012) 19839–19850.
- [21] A.K. Bhattacharya, C. Venkobachar, Removal of cadmium (II) by low cost adsorbents, *J. Environ. Eng.* 110 (1984) 110–122.
- [22] A. Schierz, H. Zänker, Aqueous suspensions of carbon nanotubes surface oxidation, colloidal stability and uranium sorption, *Environ. Pollut.* 157 (2009) 1088–1094.
- [23] H. Parab, S. Joshi, N. Shenoy, R. Verma, A. Lali, M. Sudersanan, Uranium removal from aqueous solution by coir pith: equilibrium and kinetic studies, *Bioresour. Technol.* 96 (2005) 1241–1248.
- [24] S. Li, H. Bai, J. Wang, X. Jing, Q. Liu, M. Zhang, R. Chen, L. Liu, C. Jiao, In situ grown of nano-hydroxyapatite on magnetic CaAl-layered double hydroxides and its application in uranium removal, *Chem. Eng. J.* 193–194 (2012) 372–380.
- [25] S. Azizian, Kinetic models of sorption: a theoretical analysis, *J. Colloid Interface Sci.* 276 (2004) 47–52.
- [26] Y.S. Ho, G. McKay, Pseudo-second order model for sorption processes, *Process Biochem.* 34 (1999) 451–465.
- [27] R.S. Juang, S.H. Lin, K.H. Tsao, Mechanism of sorption of phenols from aqueous solutions onto surfactant-modified montmorillonite, *J. Colloid Interface Sci.* 254 (2002) 234–241.
- [28] S.H. Choi, Y.C. Nho, Adsorption of UO₂²⁺ by polyethylene adsorbents with amidoxime, carboxyl, and amidoxime/carboxyl group, *Radiat. Phys. Chem.* 57 (2000) 187–193.
- [29] A.D. Westland, M.T.H. Tarafder, Novel peroxy complexes of uranium containing organic ligands, *Inorg. Chem.* 20 (1981) 3992–3995.
- [30] C. Prestipino, L. Regli, J.G. Vitillo, F. Bonino, A. Damin, C. Lamberti, A. Zecchina, P.L. Solari, K.O. Kongshaug, S. Bordiga, Local structure of framework Cu(II) in HKUST-1 metallocorganic framework: spectroscopic characterization upon activation and interaction with adsorbates, *Chem. Mater.* 18 (2006) 1337–1346.
- [31] J.M. Castillo, T.J.H. Vlugt, S. Calero, Understanding water adsorption in Cu-BTC metal-organic frameworks, *J. Phys. Chem. C* 112 (2008) 15934–15939.
- [32] N. Klein, I. Senkovska, K. Gedrich, U. Stoeck, A. Henschel, U. Mueller, S. Kaskel, A mesoporous metal-organic framework, *Angew. Chem. Int. Ed.* 48 (2009) 9954–9957.
- [33] M. Maes, M. Trekels, M. Boulhout, S. Schouteden, F. Vermoortele, L. Alaerts, D. Heurtaux, Y.-K. Seo, Y.-K. Hwang, J.-S. Chang, I. Beurroies, R. Denoyel, K. Temst, A. Vantomme, P. Horcajada, C. Serre, D.E. De Vos, Selective removal of n-heterocyclic aromatic contaminants from fuels by Lewis acidic metal-organic frameworks, *Angew. Chem.* 123 (2011) 4296–4300.
- [34] E. Haque, J.E. Lee, I.T. Jang, Y.K. Hwang, J.-S. Chang, J. Jegal, S.H. Jhung, Adsorptive removal of methyl orange from aqueous solution with metal-organic frameworks, porous chromium-benzenedicarboxylates, *J. Hazard. Mater.* 181 (2010) 535–542.
- [35] L. Song, J. Zhang, L. Sun, F. Xu, F. Li, H. Zhang, X. Si, C. Jiao, Z. Li, S. Liu, Y. Liu, H. Zhou, D. Sun, Y. Du, Z. Cao, Z. Gabelica, Mesoporous metal-organic frameworks: design and applications, *Energy Environ. Sci.* 5 (2012) 7508–7520.